A Special Cut-Off Gamma Camera for High-Resolution SPECT of the Head

Stig A. Larsson, Gustaf Bergstrand, Hans Bergstedt, Jan Berg, Olga Flygare, Per-Olof Schnell, Nils Andersson, and Curt Lagergren

Karolinska Hospital, S-104 01 Stockholm, Sweden, and General Electric, Nuclear Medical Aps—Jan Berg, DK 2970 Hoelrsholm, Denmark

A modern system for single photon emission computerized tomography has been modified in order to optimize examinations of the head. By cutting off part of the detector housing and collimators at one edge, it is possible to rotate the camera close to the skull while still covering the entire brain and the skull base. The minimum radius of revolution used in 32 patients was thereby reduced from about 20 cm to 12.7 ± 0.8 cm. This, combined with an adjustment of the 64 × 64 matrix to a 26- by 26-cm field of view, resulted in an improvement of the spatial resolution from about 19 mm to 12.6 ± 0.3 mm with a low-energy, all-purpose collimator, and to 10.4 ± 0.3 mm (FWHM) with a low-energy, high-resolution collimator. The improved spatial resolution offers several clinical advantages in studies of the brain, the cerebrospinal fluid space, and the skull base.

J Nucl Med 25: 1023–1030, 1984

Single photon emission computerized tomography (SPECT) has been clinically applied and found to be a useful diagnostic tool when cranial or intracranial disease is suspected. The development of rotating gamma cameras has made the technique wide spread, and its clinical usefulness has been well documented from studies of the brain (*1,2*), the cerebrospinal fluid (CSF) space (*3*), and the facial skeleton (*4–6*). The synthesis of new diffusible radiopharmaceuticals, such as I-123 IMP and I-123 HIPDM for studies of regional brain blood flow, has opened a future field of application for SPECT (*7,8*). However, the comparably low "steady state" accumulation of these tracers in the human brain (around 5% of the radioactivity administered) (*9*), has increased the need for improved techniques for routine clinical use.

Present-day rotating gamma cameras are not ideal for SPECT examinations of the head. If the entire brain or the skull base is to be covered, a rotation radius of about 20 cm must be used to permit the camera to clear the patient's shoulders. This limits the achievable spatial resolution to about 15–20 mm (FWHM), depending on the camera-to-target distance and on the collimator used (*10*).

Extensive attempts to optimize SPECT examinations of the head and brain have been made by developing special imaging devices* (*11–16*). They have all achieved a sensitivity per section and/or a spatial resolution that is superior to conventional rotating gamma cameras. However, most of the systems can acquire only a single section at a time and only very few centers have access to any of these units.

Other attempts have been made to improve rotating gamma-camera systems for studies of the brain—for example, specially designed "long-hole" collimators that improve the spatial resolution but degrade sensitivity (*17*, unpublished data, DW Palmer, JM Knoble, and BD Collier).

The use of parallel slant-hole collimators for SPECT permits reduction of the radius of rotation and thereby improves the spatial resolution in large parts of the brain (*18,19*). The holes of these collimators are slanted in only one direction, and the camera can therefore be angled and positioned close to the patient's head and shoulders in such a way that the holes lie in the transverse planes of the brain. This "low-cost" solution improves the results overall in SPECT of the head, but the spatial resolution varies in consecutive sections, and an adjustment of the transverse section width is required in order to avoid geometrical distortion in sagittal and coronal sections.

The purpose of this paper is to demonstrate the use and the properties of a newly designed "cut-off" gamma camera, which permits rotation close to the head, still covering the entire brain and the skull base. By this means, spatial resolution can be improved, relative to the results obtained with a conventional gamma camera, without any loss of sensitivity.

CAMERA DESIGN

The gamma camera used in this work is a newly designed prototype† whose detector head and collimators have been cut off at one edge (Fig. 1). The distance from the outer edge of the detector housing to the border of the circular field of view is thereby reduced from 12.5 cm (unmodified device) to 6.5 cm. The scintillator and the 61-PM-tube assembly remain unchanged, while the light guide has been slightly cut. This mechanical modification permits the detector to rotate closer to the patient's head without touching the

Received Jan. 25, 1984; revision accepted Apr. 25, 1984.

For reprints contact: Stig A. Larsson, PhD, Dept. of Hospital Physics, Karolinska Hospital, S-104 01 Stockholm, Sweden.

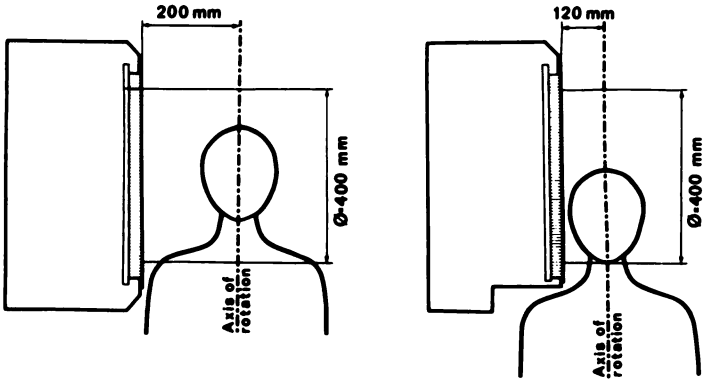

FIG. 1. Comparison of detector geometry in SPECT examinations of head with conventional gamma camera (left) and cut-off camera (right).

shoulders. The distance from the edge of the detector housing to a field of view 20 cm or more wide is 9.5 cm (with disconnection of the electronic circle-edge discriminator of the gamma camera, which rejects events outside the circular field of view). To study whether this design might be sufficient for covering the entire brain and the skull base on most patients, eight volunteers were positioned in turn, on the standard patient couch but with their heads fixed in a prototype head support (Fig. 2). The volunteers were four women and four men, ranging in height from 157 cm to 184 cm. A circular Tc-99m flood source, 40 cm in diameter, was mounted on the right side of the head. The gamma camera was positioned on the left side of the head with the collimator surface parallel with the flood source and 12 cm from the center of revolution. The couch was then moved as close as possible towards the detector housing until the camera almost touched the shoulders of the patient. A transmission image was made at that position for each volunteer in order to determine the region of the skull falling within the field of view.

The results are presented in Fig. 3. With the orbitomeatal line oriented parallel to the cut-off edge of the camera, the skull was completely covered from the top to 3.7 ± 1.2 cm below the orbitomeatal line (range 2.2–6.0 cm). An unmodified camera would not cover the entire skull, especially the base.

We conclude that both the entire brain and the skull base of most patients may be covered adequately with this prototype camera, provided that they are carefully placed within the field of view. On the other hand, the lower parts of the facial skeleton still cannot be covered with the camera rotating close to the skull.

ADJUSTMENT OF ACQUISITION MATRIX

The gamma camera used in this study has been connected to two different computers, one[§] using the Karolinska tomographic software (SPETS) (*10*), and the other a commercial system.[‡] Each of these systems is restricted to acquire data for tomographic reconstructions in 64 × 64 matrices.

When this matrix is spanned over a field of view of 40 cm diameter, the pixel width (and the associated sampling distance) becomes 6.3 mm. This matrix size is believed to be adequate for studies with 20 cm radius of rotation and a (LEAP) low energy, all-purpose collimator. However, when the radius of rotation reduces to about 12 cm, the loss of spatial resolution due to the pixel size becomes apparent and, in addition, artifacts may appear due to too coarse a sampling frequency (*10*).

For this reason, the hardware ZOOM-mode capacity of the camera system was used in order to compress the 64 × 64 matrix to a field of view of about 26 × 26 cm; thus resulting in a pixel size of about 4 × 4 mm. This pixel size corresponds effectively to a 100 × 100 matrix that is spread over the whole field of view (diam 40 cm). The position of the matrix was then adjusted to cover only the part of the field of view that is used during the examinations (Fig. 4). Unless specially indicated, all further studies in this investigation have been performed with this matrix.

SPATIAL RESOLUTION

The achievable geometrical resolving power in SPECT with

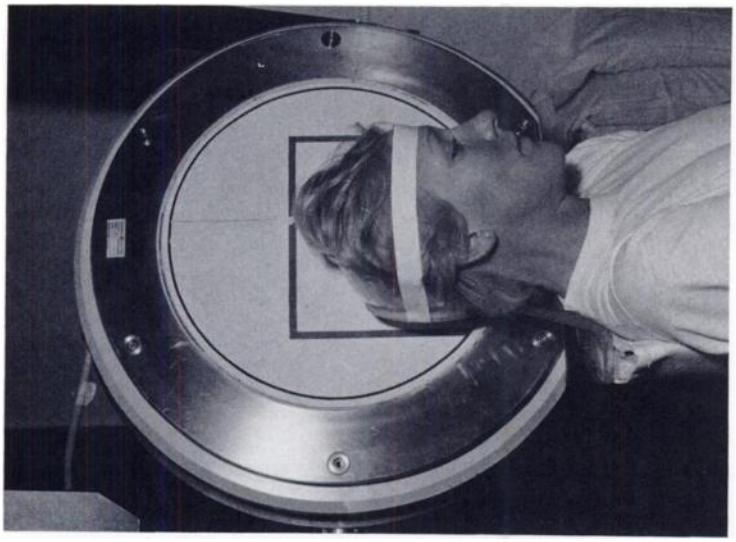

FIG. 2. Cut-off camera and patient positioned with head in prototype head holder. Square on collimator defines field of view covered by 64 × 64 matrix of this work.

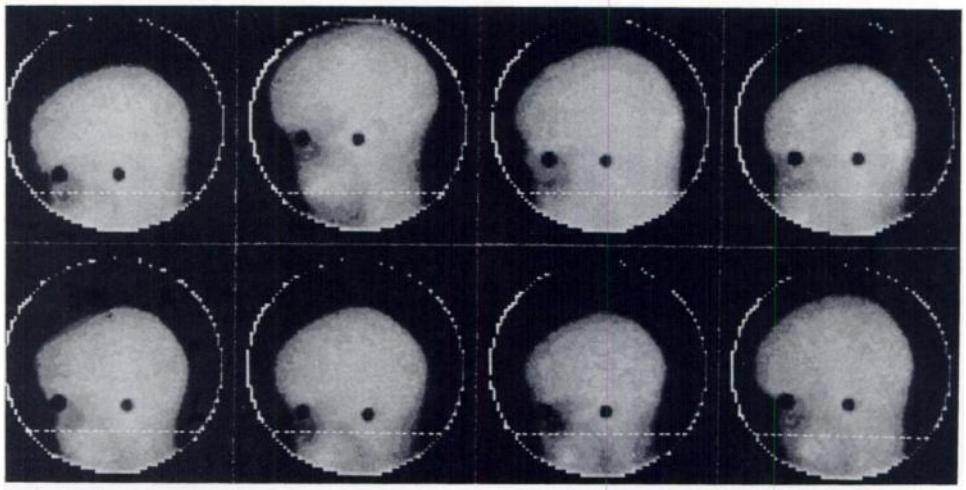

FIG. 3. Transmission images from 8 volunteers, showing region of skull being covered with camera close to head (12 cm from center of rotation). Dotted line in each image indicates lower limit of 20-cm useful field of view. The dark spots relate to Co-57 sources at lateral border of orbit and at external acoustic meatus, respectively, thus marking orbitomeatal line. Note circular boundaries; these images were acquired without disconnection of circle-edge discriminator.

rotating gamma cameras is determined essentially by the spatial resolution of the detector system (intrinsic resolution of the camera, type of collimator, and acquisition matrix), the radius of revolution, and the smoothing caracteristics of the reconstruction filter used. A rotation radius reduced from 20 to 12 cm, for instance, improved the spatial resolution from about 19 mm (FWHM) to about 14 mm (*10*). Moreover, the adjustment of the 64 × 64 acquisition matrix to the smaller field of view used in this work will contribute to a further improvement. The resulting effect on resolution was analyzed from the line source response in the projection data used for reconstruction. A Tc-99m line source, 100 mm long by 2 mm diam, was positioned within a water-filled plexiglas cylinder (diam = 215 mm, height = 185 mm) and oriented parallel to the central axis of the cylinder. The energy window was set to cover 130 to 160 keV, and the camera, equipped with a low-energy, high resolution (LEHR) collimator, was positioned at 10 cm from the wall of the cylinder. Planar images of the source were obtained at 2, 6, 10, 14, and 18 cm depth of water. The camera was then adjusted to a position 2 cm from the cylinder and all measurements were repeated.

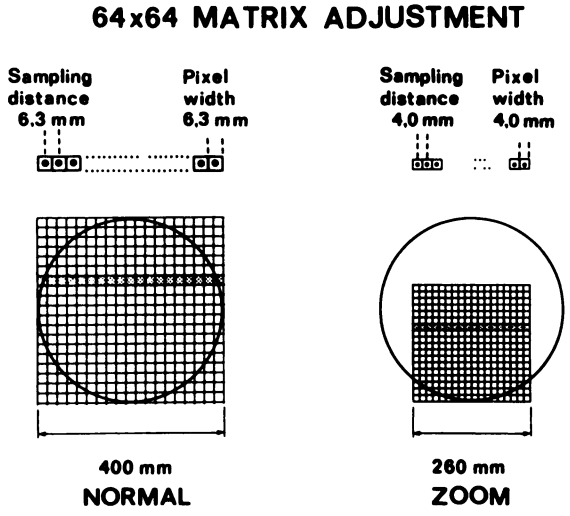

FIG. 4. Adjustment of 64 × 64 acquisition matrix to whole field of view (NORMAL) and to part (near cut-off edge) of field of view (ZOOM).

After correction for radioactive decay ($T_{1/2}$ = 6.02 hr), images corresponding to opposed projections of an object 20 cm in diameter were added together—i.e., images at 18 + 2, 14 + 6 and 10 + 10 cm. Count-rate profiles along a slice six pixels wide at the center of the line source were evaluated from these images (Fig. 5). The spatial resolution of the projection data at, for instance, 10 cm depth of water improved from 13.5 to 9.7 mm (FWHM) by decreasing the distance between the phantom and the camera, corresponding to a decrease in the radius of rotation from 20 to 12 cm.

The overall improvement of spatial resolution in reconstructed transverse sections was finally evaluated from measurements of the same line source, positioned at various distances from the center of rotation, in a 20-cm cylindrical water tank.

Tomographic images were reconstructed from measurements with rotation radii of 12 and 20 cm. All acquisitions were made at 128 equally spaced angles from 0 to 360°. Transverse sections through the center of the line source were reconstructed using the Shepp and Logan filter (*20*) (corresponding to a Hanning-weighted ramp filter with a cutoff frequency of about 1.3 cycles/pixel). Values of the FWHM and FWTM (full width at tenth maximum) are presented in Fig. 6 for the LEHR collimator. The plotted values are the means of those obtained along both the x and the y directions of the transverse plane. The spatial resolution obtained in the plane of the transverse section was 10.4 ± 0.3 mm (FWHM) at 12 cm radius of rotation and 14.2 ± 0.3 mm at 20 cm radius.

The effect of adjusting the acquisition matrix from a pixel size of 6.3 × 6.3 mm (normal mode) to one of about 4 × 4 mm (zoom mode), was investigated in the same way as in the previous study using the LEHR collimator and 12 cm orbit radius.

The results, presented in Fig. 7, show that the spatial resolution improved by almost 2 mm due to the smaller pixel size obtained by adjusting the matrix over a 26-cm field of view.

The LEHR and LEAP collimators were then compared (Fig. 8). The sensitivity of the LEHR collimator is 53% of the LEAP. The spatial resolution with the LEAP was still as good as 12.6 mm (FWHM). This means an overall improvement of about 6 mm compared with the measured resolution obtained in a previous study with a 20-cm radius of rotation and the normal 64 × 64 matrix (*10*). A summary of the values obtained at the center of the 2-cm phantom is presented in Table 1.

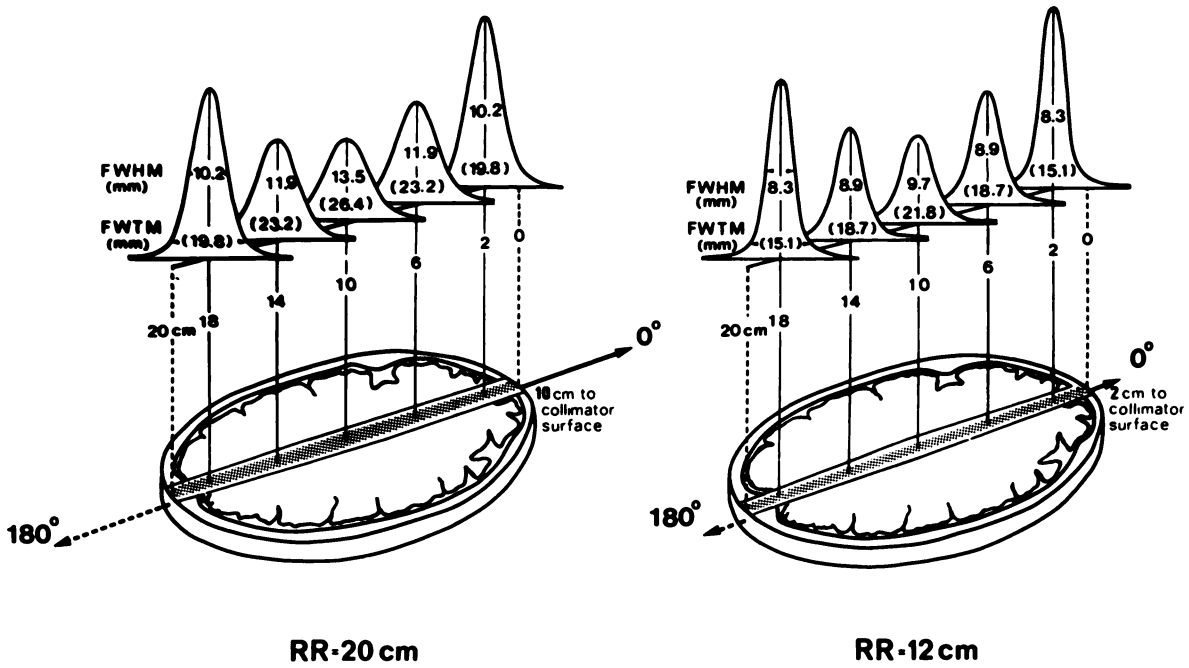

FIG. 5. Line-spread functions of opposed projection data from 20-cm-diameter object at radius of rotation of 20 cm (left) and 12 cm (right). Stippled areas in schematic brain sections below represent the FWHM, and full lines the FWTM.

PENETRATING RADIATION

Since the amount of screening lead in the cut-down wall of this prototype was reduced from 25 to 5 mm, penetrating radiation arising outside the field of view is a factor to be considered.

The penetration of low-energy photons through the reduced wall was measured and compared with the penetration through the unmodified part of the cylindrical detector shielding (lead thickness = 25 mm). A small Tc-99m source was moved stepwise in a circular orbit, 2 cm outside the cylindrical shielding of the detector. At the cut-off part of the shielding, the count rate in the energy window (130–160 keV) increased only by 0.04 cps/μCi (0.001 cps/MBq), thus demonstrating that the screening properties of the reduced wall are sufficient for low-energy photons, such as those from Tc-99m and the 159-keV photons from I-123.

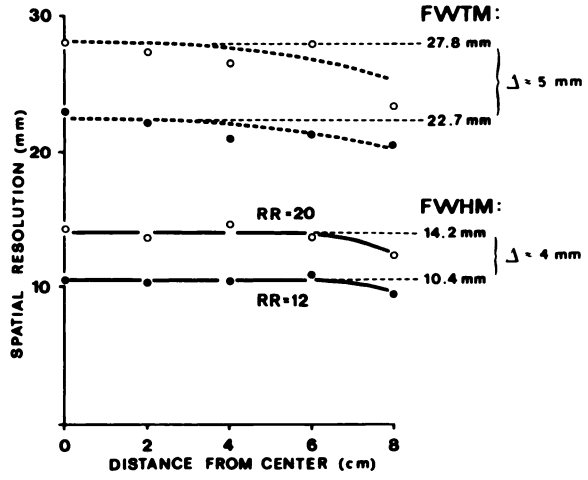

FIG. 6. Spatial resolution FWHM and FWTM as function of distance from center. Dashed curves represent FWTM and full lines represent FWHM. Closed circles represent measured values with radius of rotation (RR) of 12 cm, and open circles values obtained with RR = 20 cm.

The penetration of photons with higher energy was analysed in the same way using an I-131 source (82% at 364 keV). With an energy window spanning 330–400 keV, the count rate increased from about 0.16 cps/μCi (4.3 cps/MBq) at the unmodified wall to about 3.7 cps/μCi (100 cps/MBq) at the reduced wall—i.e. by a factor of 23. Although the number of recorded events due to penetration was closely related to the source-to-detector distance and to the position of the source along the reduced wall, and although the measurements were performed at a level where the difference in penetration was about maximum (6 cm above the front surface of the collimator), the reduced shielding of the cut-off wall makes this prototype camera unsuitable for high-energy photons.

Certain important radionuclides, such as I-123, however, may be contaminated with high-energy emitters, or may emit some high-energy photons in addition to their principal radiation. The contribution from penetrating high-energy photons in studies of I-123 (emitting 84% of photons at 159 keV and about 2% photons with energies between 347–784 keV) was analysed in a phantom study. A circular phantom 35 cm in diam (length 15 cm) was filled with a uniform solution of 5 mCi (185 MBq) I-123 in water and positioned with its central axial lying in the axis of rotation on the patient couch to simulate radioactivity within the thoracic region (outside the field of view) in a SPECT study of the head. I-124 contamination was below 0.1%.

The energy window was set for 140–190 keV and the ZOOM-mode matrix was used for acquisition. When the unmodified wall of the gamma camera was turned towards the phantom, the number of recorded events/section due to penetration was about 6,200 using a slice thickness of three pixels (nominal thickness = 12 mm) and a total acquisition time of 64 × 30 = 1920 seconds.

When the camera was adjusted for a 12-cm radius of rotation and the cut-off wall was turned towards the phantom, 17,000 counts/section were recorded during the same time. Since the number of recorded events/section from a tomographic study of regional brain blood flow with 5 mCi (185 MBq) of pure I-123 IMP may be in the range of 250,000–400,000 counts with the same examination procedure, the maximum contribution from radiation

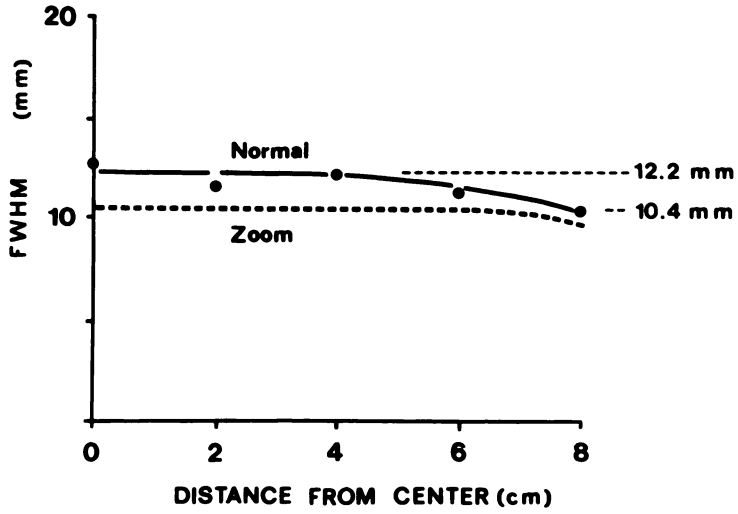

FIG. 7. Spatial resolution (FWHM) in transverse reconstructed sections using 64 × 64 acquisition matrix, extended over field of view of 40 cm (NORMAL) and 26 cm (ZOOM), respectively.

penetrating through the detector shielding would be of the order of 1.5–2.5% with an unmodified camera and 4–6% with the present prototype camera. This amount will not seriously disturb the images obtained, as is demonstrated by the clinical example in Fig. 9.

In order to ensure a better shielding against high-energy photons—for instance those originating from I-123 sources—a second version of the cut-off camera is supplied with an additional tungsten plate, 3 mm thick, and a total lead thickness of 13 mm at the cut-off edge. This improves the shielding but decreases the cut-off part slightly: from 6 cm in the present prototype to 5.5 cm in the second version.

CLINICAL EXPERIENCE

We have performed 39 examinations (26 brain studies, seven cisternographies, and six facial bone studies) in 32 patients (12 male and 20 female, mean age 46.9 yr), in addition to one study of regional brain blood flow with *N*-isopropyl-*p*-[I-123]iodoamphetamine. In these studies, the radius of rotation has varied between 11.5 and 14.5 cm (mean 12.7 ± 0.8 cm, s.d.). The LEHR collimator was used in all studies of the brain and the CSF spaces. Examinations of the facial skeleton have usually been performed with the LEAP collimator in order to achieve a reasonable number of recorded events. About 30 min before studies of the brain, 13.5 mCi (500 MBq) of [Tc-99m] pertechnetate was administered. SPECT examinations of the CSF circulation were performed 3 and 6 hr after intrathecal injection of 2.7 mCi (100 MBq) of Tc-99m DTPA (*3*). Studies of the facial skeleton were performed 3 hr after i.v. administration of 13.5 mCi (500 MBq) Tc-99m MDP. All studies were made with an acquisition time of 20 sec at each of 64 equally spaced angles between 0 and 360 degrees. In a few patients, SPECT was performed with both short and long radius of rotation in order to achieve corresponding sections for comparison. Three of these cases are presented in Figs. 10, 11, and 12. The improved image quality due to the better spatial resolution obtained when the camera is rotated close to the skull is of great importance when evaluating damage of the blood-brain barrier, CSF flow, or the extension and location of an osteogenic reaction in the skull base.

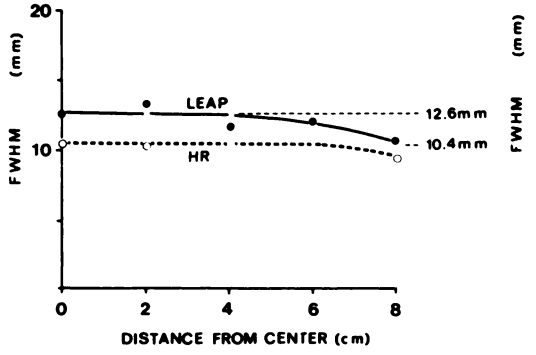

FIG. 8. Spatial resolution (FWHM) in transverse reconstructed sections obtained when using LEAP (low-energy all-purpose) and LEHR (low-energy high-resolution) collimators.

DISCUSSION AND CONCLUSIONS

The currently designed "cut-off" gamma camera permits a rotation close to the head, still retaining the entire brain and the skull base within the field of view. The spatial resolution in the tomographic sections, assessed as full width at half maximum, is thereby improved to 12.6 or 10.4 mm, depending on the choice of collimator. No modification other than a slight cut of the light guide has been made in the internal construction of the camera. Thus the physical properties of the detector head are essentially unchanged from those of a standard unit. If the lower part of the facial skeleton is to be studied with the same technique, larger modifications of the internal structure of the camera will be required.

The improved spatial resolution obtained in this work is caused mainly by minimizing the radius of rotation of the camera, but a

TABLE 1. SPATIAL RESOLUTION (mm FWHM) IN SPECT WITH 20-cm AND 12-cm ORBIT RADIUS (R)

Collimator	Matrix mode	R = 20 cm	R = 12 cm
LEAP	Normal	18.6*	14.2
LEAP	Zoom	—	12.6
LEHR	Normal	15.2*	12.2
LEHR	Zoom	14.2	10.4

* Values from Ref. (*10*) using a Maxicamera I.

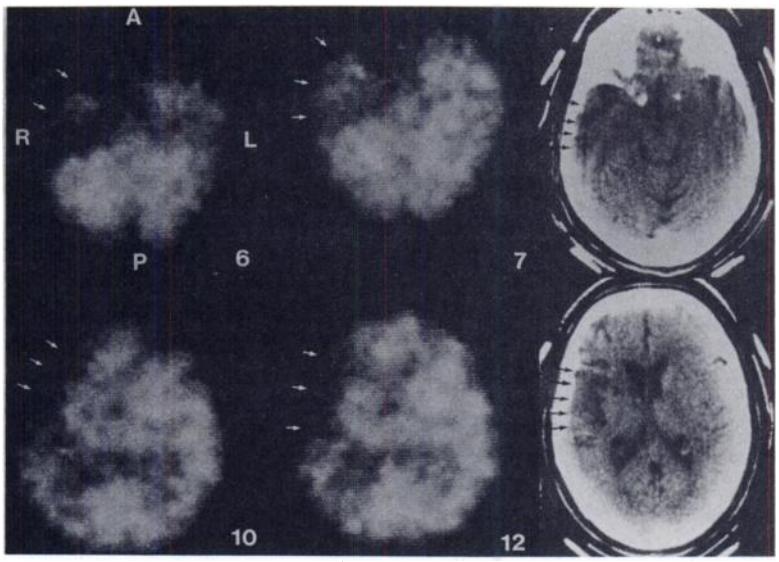

FIG. 9. SPECT and TCT examination of 53-yr-old female with right-sided occlusion of internal carotid artery. Four transverse SPECT sections at left were obtained with *N*-isopropyl-*p*-[I-123]iodoamphetamine, and demonstrate reduced blood flow to right temporal and parietal lobes (arrows). Dose administered was 5 mCi (185 MBq) and acquisition time was 30 sec for each of 64 angles using LEAP collimator. RR = 14 cm. At right are two corresponding TCT scans to demonstrate infarction in same regions (arrows).

minor part is due to the adjustment of the 64 × 64 matrix to a 26 × 26 cm field of view. This adjustment reduces the pixel size to about 4 × 4 mm, but it also increases the sampling frequency and thus the effective cut-off frequency (in cycles/mm) of the reconstruction filter. We have therefore used a filter function slightly more smoothed than that for the normal-mode matrix, in order to supress noise in the clinical images obtained with the zoomed matrix.

The circle-edge discriminator, built into in the standard system†, rejects events that are recorded outside a circle that is defined by the adjusted matrix. In the case where the 64 × 64 matrix is stretched over 26 × 26 cm, the discriminator thus rejects all events outside a circle 26 cm in diameter. This causes an unnecessary limitation of the useful field of view and makes positioning of the patient very difficult. By simple removal of the EPROM chip of the discriminator function in the camera system, it becomes possible to make use of a larger part of the whole field of view (with 40-cm diam) near the cut-off edge and a complete field of view 26 cm wide at the opposite part of the zoomed matrix. Due to edge effects, a slightly less improved spatial resolution may be obtained at the extended part of the field of view near the cut-off edge. On the other hand, serious image artifacts from radioactivity outside the field of view will essentially be avoided.

The spatial resolution in the tomographic plane alone has been considered in this study, but according to the improved resolution obtained in the projection data (Fig. 5), the decreased radius of rotation will also reduce the section width. The transverse sections of this work have all been reconstructed from a 3-pixel-wide row of the acquisition matrix, giving a nominal thickness of about 12 mm.

None of the modifications of the camera and of the electronics adopted in this work will essentially limit the use of the camera for routine clinical imaging. The shielding capacity of the cut-off wall is certainly not sufficient for high-energy photons, but the second version will have improved shielding at the reduced wall. Standard collimators with unchanged fields of view have been used, and the disconnection of the edge discriminator might influence only the count-rate properties of the camera in studies with exceptionally high count rates.

From our clinical experience so far, we recommend that future detector heads of rotating gamma cameras be modified as in our present prototype in order to permit examinations of the head under optimal conditions. In cases where improved counting statistics are of great importance, some of the improved spatial resolution might be sacrificed by using a collimator with higher sensitivity but with lower resolution.

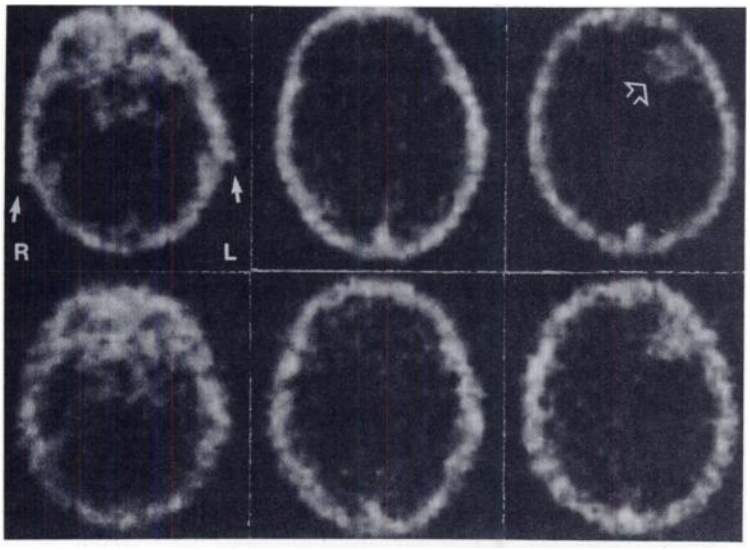

FIG. 10. SPECT studies of 76-yr-old female patient with metastasis from adenocarcinoma, performed with a radius of rotation of 12 cm (upper) and 20 cm (lower) after i.v. injection of 13.5 mCi (500 MBq) pertechnetate. Radioactivity in large vessels around sella and in transverse sinus is more easily identified in upper images than in lower. Metastasis (arrowhead) is better separated from surrounding tissues due to higher spatial resolution. Note superior portions of auricles, visible at top left (arrows).

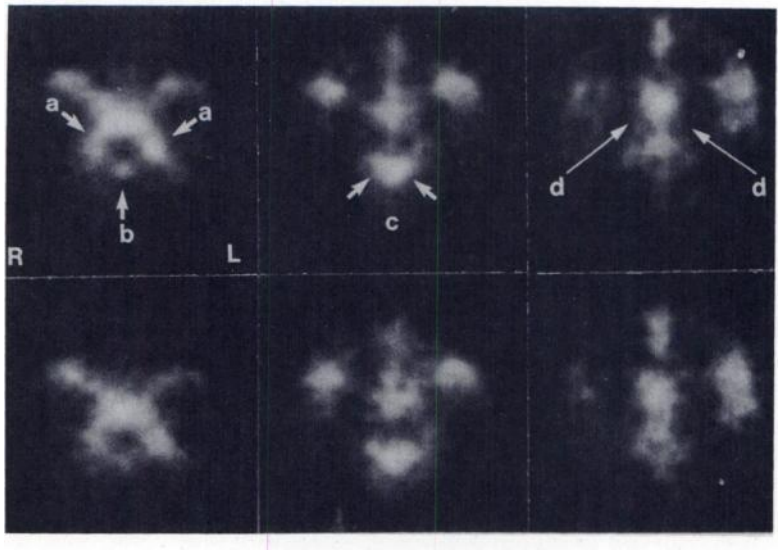

FIG. 11. SPECT of CSF spaces of 30-yr-old man. Study was performed 6 hr after intrathecal injection of 2.7 mCi (100 MBq) Tc-99m DTPA. Radioactivity in pontine angles (a), fourth ventricle (b), quadrigeminal cistern (c) and lateral ventricles (d) is clearly demonstrable in transverse sections of upper row. These sections are obtained with radius of rotation 13.5 cm; corresponding sections of lower row with radius at 22.5 cm. Differences in spatial resolution and image quality are obvious.

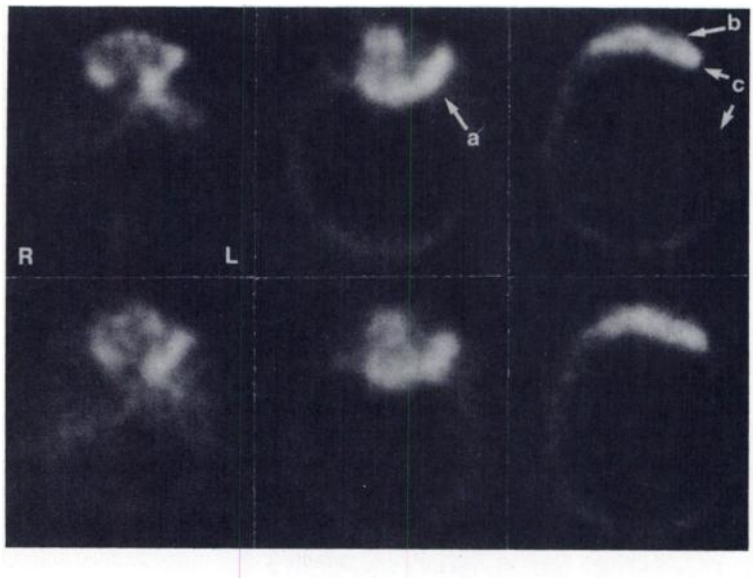

FIG. 12. SPECT of 48-yr-old female operated on for meningioma of left sphenoid ridge. Osteogenic reactions in left sphenoid wing (a) and frontal bone (b), caused by tumor recurrence or inflammatory process, and postoperative defect (c) are more precisely delineated in sections of upper row (radius of rotation = 14 cm) than in lower row (radius of rotation = 18.5 cm). Difference in radius was only 4.5 cm in this case but difference in image quality is quite clear.

FOOTNOTES

* MARK IV, CLEON (renamed as HARVARD BRAIN SCANNER, HEADTOME, SPRINT and TOMOMATIC.

† Of a Maxicamera 400 AT.

‡ General Electric Corp.

§ Digital Equipment Corp.

REFERENCES

1. KUHL DE, SANDERS TP: Comparison of rectilinear vertex and transverse section views in brain scanning. *J Nucl Med* 11:2–8, 1970
2. CARRIL JM, MAC DONALD AF, DENDY PP, et al: Cranial scintigraphy: Value of adding emission computed tomographic sections to conventional pertechnetate images (512 cases). *J Nucl Med* 20:1117–1123, 1979
3. BERGSTRAND G, LARSSON S, BERGSTRÖM M: Cerebrospinal fluid circulation: Evaluation by single-photon and positron emission tomography. *Am J Neuroradiol* 4:557–559, 1983
4. BROWN ML, KEYES JW, LEONARD PF, et al: Facial bone scanning by emission tomography. *J Nucl Med* 18:1184–1188, 1977
5. ELL PG, KAHN O: Emission computerized tomography: Clinical applications. *Semin Nucl Med* 11:50–60, 1981
6. BERGSTEDT H, ISRAELSSON A, LARSSON S, LIND M: Computerized emission tomography of the facial skeleton and skull base. BRH-publ (FDA 81-8177), 177–180, 1981
7. KUHL DE, WU JL, LIN TH, et al: Mapping local cerebral blood flow by means of emission computed tomography of N-isopropyl-p(I-123)-iodoamphetamine (IMP). *J Nucl Med* 22:P16, 1981 (abst)
8. HILL TC, HOLMAN LB, LOVETT R, et al: Initial experience with SPECT (single photon computerized tomography) of the brain using N-isopropyl I-123 p-iodoamphetamine: Concise communication. *J Nucl Med* 23:191–195, 1982
9. KUHL DE, BARRIO JR, HUANG SC, et al: Quantifying local cerebral blood flow by N-isopropyl-p-[I-123]-iodoamphetamine (IMP) tomography. *J Nucl Med* 23:196–203, 1982
10. LARSSON SA: Gamma camera emission tomography. De-

velopment and properties of a multi-sectional emission computed tomography system. *Acta Radiol Suppl* 363:1-75, 1980

11. KUHL DE, EDWARDS RQ, RICCI AR, et al: The MARK IV system for radionuclide computed tomography of the brain. *Radiology* 121:405-413, 1976
12. STODDART HF, STODDART HA: A new development in single gamma transaxial tomography. Union Carbide focused collimator scanner. *IEEE Trans Nucl Sci* NS-26:2710-2712, 1979
13. ZIMMERMAN RE, KIRSCH CM, LOVETT R, HILL TC: Single photon emission computed tomography with short focal length detectors. In *Single Photon Emission Computed Tomography and Other Selected Topics*. Sorenson JA, ed. New York, Society of Nuclear Medicine, 1980, 147-157.
14. KANNO I, VEMURA K, MIURA S, et al: HEADTOME: A hybrid emission tomograph for single photon and positron emission imaging of the brain. *J Comp Assist Tomogr* 5: 216-226, 1981
15. ROGERS WL, CLINTHORNE NH, STAMOS J, et al: SPRINT: A single photon ring tomograph. *J Nucl Med* 23: P59, 1982 (abst)
16. STOKELY EM, SVEINSDOTTIR E, LASSEN NA, et al: A single photon dynamic computer assisted tomograph (DCAT) for imaging brain function in multiple cross sections. *J Comp Assist Tomogr* 4:230-240, 1980
17. KIRCOS LT, LEONARD PF, KEYES JW: An optimized collimator for single-photon computed tomography with a scintillation camera. *J Nucl Med* 19:322-323, 1978
18. LARSSON SA: Single photon emission computed tomography—current status, limitations and applications. 2nd International symposium on fundamentals of technical progress in medicine. Liege, Belgium pV.7, 1-13, 1983
19. POLAK JF, HOLMAN BL, MORETTI JL, et al: I-123 HIPDM brain imaging with a rotating gamma camera and slant-hole collimator. *J Nucl Med* 25:495-498, 1984
20. SHEPP LA, LOGAN BF: The Fourier reconstruction of a head section. *IEEE Trans Nucl Sci* NS-21:21-43, 1974